

# Analysis of the Effect of Thermal Expansion of Metals on the Stability of the Metal Cutting Process

Victor P. Lapshin \*

*Don State Technical University, faculty of Automation, Mechatronics and Control, Department of Automation of Production Processes, 344002 Rostov-on-Don, Russia.*

Received 7 Jan 2023

Accepted 24 Jun 2023

## Abstract

One of the most important problems that largely determine the effectiveness of modern metal cutting control systems is the problem of ensuring such cutting modes in which the durability of the cutting tool will be maximum. In this article, a new mathematical apparatus is proposed that allows linking the stability of the dynamics of the cutting process with the predicted residual durability of the cutting tool. The aim of the study is to develop a methodology for determining the best processing speed mode, which ensures maximum stability of the cutting system in the space of processing speed parameters and the degree of wear of the cutting wedge. The study consists of a series of experiments on the STD201-1 measuring stand, as well as modeling in the Matlab mathematical software package. Based on this, the main method underlying the research is the method of numerical modeling in the Matlab environment. The results show that the most important factor limiting the stability of the cutting system in the space of the parameters of the processing speed and the degree tool wear is the factor of thermal expansion of the cutting metal being processed.

© 2023 Jordan Journal of Mechanical and Industrial Engineering. All rights reserved

**Keywords:** cutting process; thermodynamics; tool wear; vibrations; process stability.

## 1. Introduction

The most important factor determining the quality of the metal cutting process on metal-cutting machines, as well as the durability of the cutting tool, is the factor of the cutting process dynamics stability. Despite the development of modern control systems for cutting processes on metal-cutting machines, which organically absorb almost all achievements of scientific and engineering thought, the vibrational activity of the tool remains a problem in metalworking today. The vibrations of the tool accompanying the cutting process are largely determined by the regeneration of vibrations when cutting along the “trace”, what was called the regenerative effect [1-6]. In general, it was found that the main factor influencing the regenerative effect is the so-called time delay [7], that is why it has a decisive effect on the stability of the process dynamics. In addition to the regenerative nature of self-excitation of the cutting system vibration dynamics, the vibration stability of the cutting tool is affected by: the temperature in the contact zone of a tool and a workpiece [8], changes in the force reaction from the cutting process to the shaping movements of the tool [9], the value characterizing the degree of wear of the cutting wedge, etc. [10].

All enumerated above determine the vibration stability of the cutting control system, which means its ability to respond to limited control and disturbing effects in a limited way. At the same time, the higher the stability margin of cutting

system dynamics, the more limited the vibration response of the system will be, and the lower the vibrations of the cutting wedge are, the better the quality of the surface to be treated and, in many ways, the greater the residual resistance of the tool. In this regard, the task arises of synthesizing current mathematical models of cutting processes dynamics and the methodology for determining the assessment of the stability reserves of cutting systems based on them.

Mathematical models of cutting control systems in metalworking have the property of nonlinearity and at the same time are quite complex, since the cutting force and cutting temperature are nonlinear functions of the deformation displacements coordinates of the tool [11], in which such evolutionary characteristics as the wear of the cutting tool are important factors [12]. In the work of V. P. Astakhov [13], the relationship between the cutting temperature and the wear of the cutting tool is described, the relationship of vibrations, temperature and the evolution of the cutting wedge is shown here. The interconnectedness of the cutting process through the disclosure of its evolutionary changes is examined more deeply in the works [14] and [12]. One of the factors of the complexity of the model is taking into account the time delay in the formation of the area of the cut layer. Here I will note that in the process of linearization of a system of equations, we will have to deal with an element containing a lagging argument. Such an element will not allow an analysis of the system of differential equations of the cutting control system using a linearized model in the

\* Corresponding author e-mail: lapshin1917@yandex.ru

vicinity of the equilibrium point based on algebraic criteria, such as Hurwitz criterion [15] or Raus criterion [16].

As a solution to the problem outlined above, the use of frequency stability criteria, such as the Nyquist criterion [17-18], or its Soviet counterpart, the Mikhailov criterion [19-21], can be used. The Nyquist criterion itself, applied to mathematical models of metal cutting control systems, is well considered in the works of V.L. Zakorotny [11], but Mikhailov's criterion, well-known in the American engineering school for a long time [21], has not been widely used today in solving problems of dynamics of cutting control systems on metal-cutting machines.

In the works of famous specialists in the field of metalworking, among other things, the fact of the existence of some best processing mode associated with the cutting speed is noted [22-23]. In these works, the optimal mode is understood as ensuring the minimum roughness of the treated surface and the maximum dimensional stability of the cutting tool. For example, A.D. Makarov, in his monograph [22], formulates the following statement: "the most important factor determining the characteristics of the cutting process is the average contact temperature determined by the cutting mode (processing speed)". In this and other works, the tool contact temperature is determined by the current power released during the cutting and converted into heat, which linearly depends on the cutting speed. However, in the article [8] published in Materials, it was proved that during the formation tool wear along the back face, an additional thermodynamic feedback is formed, which pre-warms the cutting zone for the period up to the current moment of cutting. Such heating will lead to a thermal expansion of workpiece material, which will increase the value of the force pushing the tool. This factor, the restructuring of the force reaction, which is confirmed by experimental studies [9], was not previously taken into account when forming mathematical models of cutting systems.

In this regard, the aim of the study was to assess the influence of the thermal expansion of metals associated with the evolution of the cutting wedge (wear) on the stability of the vibration dynamics of metal cutting control systems in metal-cutting machines, with the development of a methodology for assessing stability based on the Mikhailov frequency criterion.

**2. Research methodology**

*2.1. Experiment at the stand STD. 201-1*

Preliminary heating of the cutting zone, as a result of the energy transfer mechanism action identified in the work [8], will lead to the thermal expansion of the processed workpiece material, which will affect the value of the pushing force. To determine the dependence of the buoyant force on the magnitude of the contact temperature of the tool and the workpiece, a series of experiments were carried out using the experimental setup STD.201-1 (STD - System of technical diagnosis), which involves adjusting the weight coefficients to calculate the cutting temperature based on the values of the removed natural thermal electromotive force (EMF) STD. STD.201-1 measures the force along the axes of deformation, temperature and vibration. To do this, the research methodology provides for a whole setup procedure, which includes a double measurement of the contact temperature, a

measurement using a natural thermal EMF and measurements carried out next to the contact with a calibrated thermocouple. The connection example for the case of measuring the effect of contact temperature on the buoyant force, for the case of steel 45, is shown in Figure 1.

As a tool, the holder MR TNR 2020 K11 and a five-sided plate 10113-110408 T15K6 were used, with an angle in the upper part (angle of attack)  $\gamma_0 = 35^\circ$ , the main angle in terms of  $\varphi = 80^\circ$ .

The measurement results are presented by the software interface of the system, the external view of which is shown in Figure 2.

The results of experiments to assess the influence of the contact temperature on the value of the force pushing the tool out of the cutting zone, for the case of processing steel 45, are shown in Table 1.

**Table 1.** experiments contact steel 45

Steel	C	Si	Mn	Cr	Ni	Ti	S	P
12X18H10T	0,42-0,50	0,17-0,37	0,50-0,80	0,030	0,035	0,25	0,30	0,30

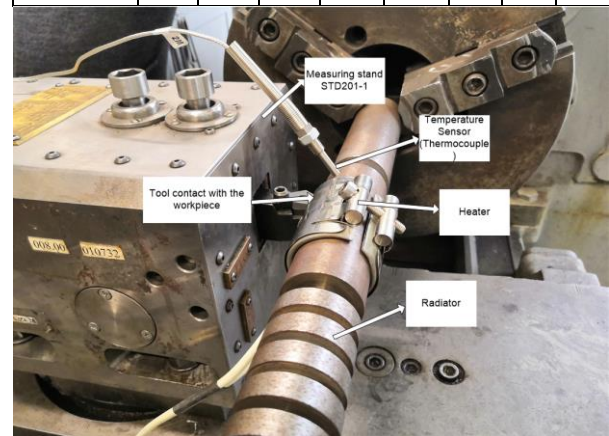


**Figure 1.** Experimental setup prepared to assess the effect of contact temperature on the buoyant force

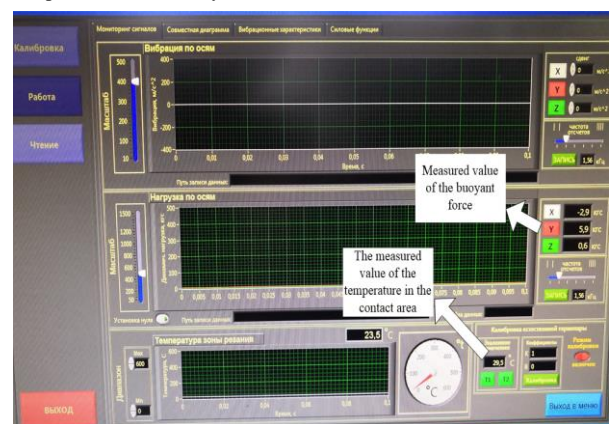


**Figure 2.** Interface of the stand STD201-1

A graphical representation of the experimental results presented in Table 2 is shown in Figure 3.

**Table 2.** Dependence of  $F_y$  on contact temperature

Q, °C	30	40	50	60	70	80	90	100	110	120	130
$F_y$ , N	9.5	9.7	10.3	10.9	11.5	12.2	12.8	13.4	13.8	14.3	14.6

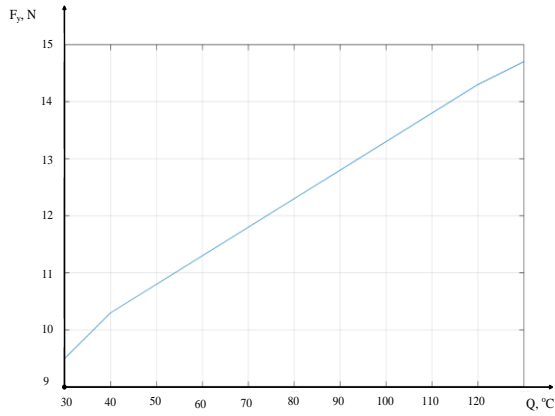


Figure 3. Results of the experiment on steel 45

As can be seen from the Figure 3, the buoyant force almost linearly depends on the contact temperature, which is quite understandable from the point of view of the linear nature of metals expansion with the increase in their temperature. The average coefficient of linear increases in the buoyant force with the increase in the contact temperature  $k_Q^F$ , for the case of steel 45, was 0.05625.

A similar experiment was conducted for the case, when the processed part is heat-resistant and heat-resistant steel 12X18H10T.

Table 3. Химический состав стали 12X18H10T

Steel	C	Si	Mn	Cr	Ni	Ti	S	P
12X18H10T	0,12	0,80	2,00	17,0-19,0	9,0-11,0	5,0-8,0	0,02	0,40

The results of the experiment to determine buoyant force for steel case 12X18H10T, they are shown in Table 4 and in Figure 4.

Table 4. Dependence of  $F_y$  on contact temperature

Q, °C	30	40	50	60	70	80	90	100	110	120	130
$F_y$ , N	9.1	9.6	10.3	11	11.4	11.8	12.1	12.5	12.9	13.2	13.6

A graphical representation of the experimental results presented in Table 4 is shown in Figure 4.

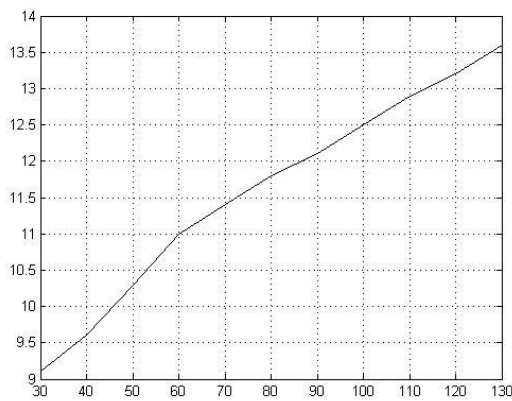


Figure 4. Results of the experiment on steel 12X18H10T

The experiments have shown that the buoyant force, when cutting linearly depends on temperatures of the processed part for steel 12X18H10T it also amounted to 0.04231.

2.2. Basic Mathematical Model Synthesis

For an adequate interpretation of the synthesized model, we should consider the diagram of force reaction decomposition from the cutting process to the movements of the forming tool along the axes of deformation of this tool during the turning (see Figure 4).

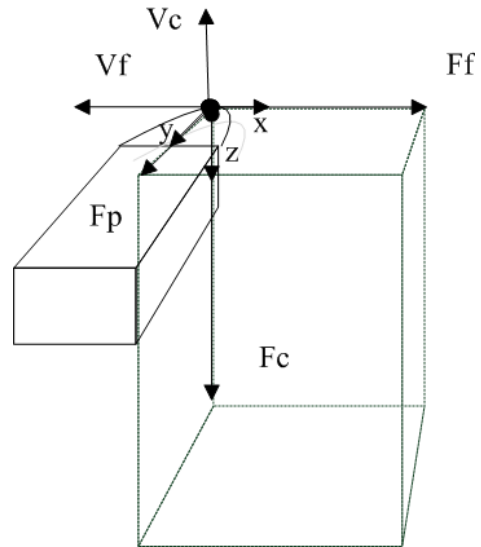


Figure 4. The structure of axes and forces

In the diagram (Figure 4): x-axis—the axial direction of deformations (mm), y-axis—the radial direction of deformations (mm), and z-axis—the tangential direction of deformations (mm). Along the same axes, the force response is decomposed from the cutting process to the shaping motions of the tool ( $F_f, F_p, F_c$  (N)),  $V_f$  and  $V_c$  (mm/s) of the feed and cutting speeds.

It is convenient to interpret the dependence of the cutting force on the temperature-speed factor of cutting in the form of a falling exponential dependence, as it is presented in the formula below:

$$\rho = \rho_0 \left( 1 + \mu e^{-\alpha_\mu \left( V_c - \frac{dz}{dt} \right)} \right), \tag{1}$$

where  $\rho_0$  is a certain minimum value of the coefficient  $\rho$  (the coefficient characterizing the chip pressure on the front face of the cutting wedge),  $\mu$  is the coefficient showing the increase of the value  $\rho$  to a certain maximum value,

$\alpha_\mu$  is the coefficient of the value drop steepness  $\rho$ ,  $\left( V_c - \frac{dz}{dt} \right)$  is the instantaneous cutting speed.

Taking into account the formula (1), as well as relying on the hypothesis of the cutting force proportionality of the cut layer area, the cutting force will be interpreted as:

$$F = \rho_0 \left( 1 + \mu e^{-\alpha_\mu \left( V_c - \frac{dz}{dt} \right)} \right) (a_p - y) \int_{t-T_v}^t \left( V_f - \frac{dx}{dt} \right) dt \tag{2}$$

where  $(a_p - y)$  - instantaneous cutting depth,

$\int_{t-T_v}^t \left( V_f - \frac{dx}{dt} \right) dt$  - real feed.

The ejecting force, an instrument from the cutting zone, depending on the wear of the tool along the back face, and

depending on the temperature expansion of the processed material, we consider as:

$$F_h = (\sigma_0 + k_Q^F Q_h) h_3 (a_p - y) e^{-K_h x}, \quad (3)$$

where  $\sigma_0$  is the tensile strength of the processed metal under compression in  $[kg/mm^2]$ , at the contact temperature along the back face of the tool and the workpiece  $Q_h$  at zero degrees Celsius,  $K_h$  is the coefficient characterizing the nonlinear build-up of the pushing force when the back face of the tool and the workpiece become closer.

Through the main angle in the plan -  $\varphi$ , it is possible to decompose the buoyant force on the deformation axes  $x$  and  $y$ , as follows:

$$\begin{cases} F_h^{(x)} = \cos \varphi F_h \\ F_h^{(y)} = \sin \varphi F_h \end{cases}. \quad (4)$$

The force reaction on the back face of the tool in the direction of  $z$  coordinate is represented by the friction force, which can be represented as:

$$F_h^{(z)} = k_t F_h, \quad (5)$$

where  $k_t$  is the coefficient of friction, which, based on the reasoning given in [22], can be interpreted as:

$$k_t = k_{0t} + \Delta k_t [e^{-K_{f1} Q_h} + e^{K_{f2} Q_h}] / 2, \quad (6)$$

$$\begin{cases} m \frac{d^2 x}{dt^2} + h_{11} \frac{dx}{dt} + h_{12} \frac{dy}{dt} + h_{13} \frac{dz}{dt} + c_{11} x + c_{12} y + c_{13} z = F_f \\ m \frac{d^2 y}{dt^2} + h_{21} \frac{dx}{dt} + h_{22} \frac{dy}{dt} + h_{23} \frac{dz}{dt} + c_{21} x + c_{22} y + c_{23} z = F_p \\ m \frac{d^2 z}{dt^2} + h_{31} \frac{dx}{dt} + h_{32} \frac{dy}{dt} + h_{33} \frac{dz}{dt} + c_{31} x + c_{32} y + c_{33} z = F_c \end{cases}, \quad (8)$$

where  $m$   $[kg \cdot s^2/mm]$ ;  $h$   $[kg \cdot s/mm]$ ;  $c$   $[kg/mm]$  – matrices of inertia coefficients, dissipation coefficients and stiffness coefficients, respectively.

where  $k_{0t}$  is a constant minimum value of the coefficient of friction,  $\Delta k_t$  is the value of the increment of the coefficient of friction with a change in temperature in the contact zone,  $K_{f1}$  and  $K_{f2}$  the coefficients determining the steepness of the fall and growth of the coefficient of friction characteristics.

As the generalization of the force reaction from the cutting process to the shaping movements of the tool (see Figure 4), we obtain the following equations describing the force reaction:

$$\begin{cases} F_f = \chi_1 F + F_h^{(x)} \\ F_p = \chi_2 F + F_h^{(y)} \\ F_c = \chi_3 F + F_h^{(z)} \end{cases}, \quad (7)$$

where  $\chi_i$  is a certain coefficient of general vector decomposition of reaction forces on the  $i$ -th axis of tool deformation, it should be noted here that this approach is widely used within the scientific school of Zakorotny V.L. [10].

The model of deformation movements of the tool tip, based on the approach used in the scientific school of Zakorotny V.L. [10, 11, 17], will have the following form:

The differential equation describing the transfer of temperature through the back face of the tool at the previous rotation of the spindle to the current contact zone of the tool and the workpiece [8] will take the following form: The differential equation describing the transfer of temperature through the back face of the tool at the previous rotation of the spindle to the current contact zone of the tool and the workpiece [8] will take the following form:

$$T_1 T_2 \frac{d^2 Q_h}{dt^2} + (T_1 + T_2) \frac{dQ_h}{dt} + Q_h = kN,$$

Where  $T_1, T_2$  - time constants,  $k$  - transfer factor,  $N$  - allocated power:

$$N = F_c(t - T_v) \left( V_c - \frac{dz(t - T_v)}{dt} \right) = (\chi_3 F(t - T_v) + F_h^{(\varepsilon)}(t - T_v)) \left( V_c - \frac{dz(t - T_v)}{dt} \right) \quad (10)$$

Thus, the system of equations (8) and the differential equation (9), taking into account equations (7) and (10), will represent a mathematical model of the dynamics of the cutting system.

### 2.3. The Mikhailov criterion and linearization of the mathematical model

To assess the stability of the control system based on the Mikhailov criterion, the characteristic polynomial of the transfer function of the control system is used:  $D(p) = a_0 p^n + a_1 p^{n-1} + \dots + a_{n-1} p + a_n$ , where  $n$  is the degree of polynomial and it is also the order of the differential equation, for our case it is  $n=8$ . Assuming that  $p = j\omega$ , we transform the characteristic polynomial into a complex frequency polynomial:  $D(j\omega) = a_0(j\omega)^n + a_1(j\omega)^{n-1} + \dots + a_{n-1}(j\omega) + a_n$ . Depending on the degree of the number  $(j\omega)^n$ , it is either real or imaginary. For this reason, the frequency polynomial splits into the real part  $U(\omega)$  and the imaginary part  $V(\omega)$ , where  $U(\omega)$  is an even function of  $\omega$ ,  $V(\omega)$  is an odd function of  $\omega$ .

By setting any value of the frequency  $\omega$ , we get the numbers  $U(\omega)$  and  $V(\omega)$ . Together they form a complex number  $D(j\omega)$ . On the complex plane, it is denoted by the point  $M(U,V)$ . The set of points  $M(U,V)$  corresponding to different frequencies form a curve called the Mikhailov hodograph.

In the case of stable systems, the Mikhailov hodograph has the property of starting from the point  $U(0) = a_n, V(0) = 0$ . As  $\omega$  increases from zero to infinity, the point  $M(U,V)$  moves to the left so that the curve tends to cover the origin of coordinates, while moving away from it. If we draw the radius vector from the origin to the point  $M(U,V)$ , it turns out that the radius vector will rotate counterclockwise, continuously increasing.

The Mikhailov criterion itself can be summarized as follows: if the frequency changes from zero to infinity, the Mikhailov hodograph starts on the real axis at the point  $a_n$ , sequentially passes counterclockwise  $n$  quadrants of the complex plane without passing through zero, and goes to infinity in the  $n$ -th quadrant, the system is stable. In the case of unstable systems, the curves do not cover the origin of coordinates, while the hodograph starts from the origin or passes through the origin, the system is on the boundary stability [18-20].

Thus, to assess the stability of the control system, it will be necessary to determine the characteristic polynomial of the control system described by a system of differential equations of the eighth order (system of equations (9) and equation (10)). As this system is nonlinear, it will be necessary to linearize this system of equations in some vicinity of the equilibrium point. For subsequent analysis, it will be necessary to switch to the operator form of a linearized system writing, that is, to perform the Laplace transformation, assuming that the initial conditions are zero ( $p$  is the Laplace transform operator, under zero initial conditions  $p = \frac{d}{dt}$ ). After all mentioned above, it is possible

to present a linearized system of differential equations in matrix-vector form:

$$\begin{cases} a_{11}(p)x(p) + a_{12}(p)y(p) + a_{13}(p)z(p) + a_{14}(p)Q_h(p) = 0 \\ a_{21}(p)x(p) + a_{22}(p)y(p) + a_{23}(p)z(p) + a_{24}(p)Q_h(p) = 0 \\ a_{31}(p)x(p) + a_{32}(p)y(p) + a_{33}(p)z(p) + a_{34}(p)Q_h(p) = 0 \\ a_{41}(p)x(p) + a_{42}(p)y(p) + a_{43}(p)z(p) + a_{44}(p)Q_h(p) = 0 \end{cases} \quad (11)$$

where the coefficients of matrix are

$$A = \begin{pmatrix} a_{11}(p) & a_{12}(p) & a_{13}(p) & a_{14}(p) \\ a_{21}(p) & a_{22}(p) & a_{23}(p) & a_{24}(p) \\ a_{31}(p) & a_{32}(p) & a_{33}(p) & a_{34}(p) \\ a_{41}(p) & a_{42}(p) & a_{43}(p) & a_{44}(p) \end{pmatrix}, \quad (12)$$

$a_{ij}, i=1..4, j=1..4$ , are represented by the following formulas:

$$\left\{ \begin{aligned}
 a_{11}(p) &= mp^2 + h_{11}p + \chi_1(1 - e^{-jT_v\omega})\rho_0^V t_p + \cos(\varphi)K_h\sigma_0 h_3 t_p + c_{11} \\
 a_{12}(p) &= h_{12}p + \chi_1\rho_0^V S_0 + \cos(\varphi)\sigma_0 h_3 + c_{12} \\
 a_{13}(p) &= h_{13}p - p\chi_1\rho_0\mu\alpha_1 t_p S_0 + c_{13} \\
 a_{14}(p) &= \cos(\varphi)k_Q^h h_3 t_p \\
 a_{21}(p) &= h_{21}p + \chi_2(1 - e^{-jT_v\omega})\rho_0^V t_p + \sin(\varphi)K_h\sigma_0 h_3 t_p + c_{21} \\
 a_{22}(p) &= mp^2 + h_{22}p + \chi_2\rho_0^V S_0 + \sin(\varphi)\sigma_0 h_3 + c_{22} \\
 a_{23}(p) &= h_{23}p - p\chi_2\rho_0\mu\alpha_1 t_p S_0 + c_{23} \\
 a_{24}(p) &= \sin(\varphi)k_Q^h h_3 t_p \\
 a_{31}(p) &= h_{31}p + \chi_3(1 - e^{-jT_v\omega})\rho_0^V t_p + c_{31} + K_h\sigma_0 h_3 t_p (k_{0t} + \Delta k_t) \\
 a_{32}(p) &= h_{32}p + \chi_3\rho_0^V S_0 + c_{32} + \sigma_0 h_3 (k_{0t} + \Delta k_t) \\
 a_{33}(p) &= mp^2 + h_{33}p - p\chi_3\rho_0\mu\alpha_1 t_p S_0 + c_{23} \\
 a_{34}(p) &= k_Q^h h_3 t_p (k_{0t} + \Delta k_t) + (K_{f2} - K_{f1})\Delta k_t \sigma_0 h_3 t_p \\
 a_{41}(p) &= k[\chi_3(1 - e^{-jT_v\omega})e^{-jT_v\omega}\rho_0^V t_p V_c + K_h\sigma_0 h_3 t_p (k_{0t} + \Delta k_t)e^{-jT_v\omega}V_c] \\
 a_{42}(p) &= k[\chi_3 e^{-jT_v\omega}\rho_0^V S_0 V_c + \sigma_0 h_3 (k_{0t} + \Delta k_t)e^{-jT_v\omega}V] \\
 a_{43}(p) &= kp[(\chi_3\rho_0^V S_0 + \sigma_0 h_3 t_p (k_{0t} + \Delta k_t))e^{-jT_v\omega} - e^{-jT_v\omega}\chi_3\rho_0\mu\alpha_1 t_p S_0 V_c] \\
 a_{44}(p) &= T_1 T_2 p^2 + (T_1 + T_2)p + 1 - k(k_Q^h h_3 t_p (k_{0t} + \Delta k_t) + \\
 &+ (K_{f2} - K_{f1})\Delta k_t \sigma_0 h_3 t_p)e^{-jT_v\omega}V_c
 \end{aligned} \right. \tag{13}$$

Now we will move to the time domain by replacing  $p = j\omega$ , after which the characteristic polynomial of the control system will be represented as the determinant of the matrix A given in expression (12). It means that the characteristic polynomial of the control system and the Mikhailov vector is represented as follows:

$$D(j\omega) = \det(A(j\omega)) = \begin{vmatrix} a_{11}(j\omega) & a_{12}(j\omega) & a_{13}(j\omega) & a_{14}(j\omega) \\ a_{21}(j\omega) & a_{22}(j\omega) & a_{23}(j\omega) & a_{24}(j\omega) \\ a_{31}(j\omega) & a_{32}(j\omega) & a_{33}(j\omega) & a_{34}(j\omega) \\ a_{41}(j\omega) & a_{42}(j\omega) & a_{43}(j\omega) & a_{44}(j\omega) \end{vmatrix} \tag{14}$$

Thus, the equation (14) is the Mikhailov vector, which hodograph is under the study on the complex plane when the frequency  $\omega$  changes from zero to infinity.

### 3. Modeling results and discussion

For the convenience of interpreting the results of numerical experiments, the simulation was carried out in the Matlab/Simulink 2014 package, where the system of equations (8-9) was directly modeled in Simulink, and the Mikhailov vector represented by expression (14) was calculated in a separate cycle in Matlab 2014 itself, where at every step of the cycle the determinant for a specific value of the frequency  $\omega$

was considered, and the given value was postponed to the complex plane, then everything was repeated. In general, the value for  $\omega$  was calculated from zero to 4000 Hz in increments of 0.01 Hz. The simulation results are shown below in a number of figures.

To assess the stability of the cutting control system by the Mikhailov method, the variants of the control system, the variant of a stable and the variant of an unstable (at the boundary of stability) system were considered. As a factor affecting the stability of the cutting process, the amount of tool wear along the back face ( $h_3$ ) was used. On the basis of the Mikhailov criterion, the boundary of the stability area of the cutting management system was estimated in the processing speed (revolutions per minute) and the amount of wear (mm). In total, twenty possible cutting speed modes were investigated, in each of which the dynamics of the control system and the hodograph of Vector Mikhailov were considered for five possible values of the wear value of the cutting wedge along the rear face, three variants characterize the stable dynamics of the cutting system, one variant -stability boundary and one variant -unstable behavior of the system.

The parameters of the simulated control system were as follows:

$$m = \begin{bmatrix} 0,0065 & 0 & 0 \\ 0 & 0,0065 & 0 \\ 0 & 0 & 0,0065 \end{bmatrix} \text{ kg} \cdot \text{s}^2 / \text{mm};$$

$$h = \begin{bmatrix} 0,844 & 0,39 & 0,37 \\ 0,39 & 0,77 & 0,36 \\ 0,37 & 0,36 & 0,75 \end{bmatrix} \text{ kg} \cdot \text{s} / \text{mm};$$

$$c = \begin{bmatrix} 1390 & 190 & 165 \\ 190 & 795 & 150 \\ 165 & 150 & 970 \end{bmatrix} \text{ kg} / \text{mm}. \text{ Tool orientation}$$

coefficients:

$$\chi_1 = 0,3369, \quad \chi_2 = 0,48, \quad \chi_3 = 0,81.$$

Technological modes: depth  $a_p = 1\text{mm}$ , submission for

$$\text{turnover } fr = 0,11\text{mm/turnover}, \quad \rho_0 = 400 \frac{\text{kg}}{\text{mm}^2},$$

radius of the workpiece  $R = 25\text{mm}$ , the main angle in the plan  $\varphi = 80^\circ$ . Matrices of stiffness coefficients and dissipation coefficients were obtained in a series of preliminary tests on experimental equipment during calibration of the stand STD. 201-1.

A variant of a stable cutting system for a variant of a system with a processing speed of 820 revolutions per minute and a wear value of 0.22 mm, in the form of transient characteristics of the deformation coordinates when the tool is embedded in the workpiece and the corresponding phase trajectories, are shown in Figure 5.

As can be seen from Figure 5, for the case of cutting with a frequency of 820 revolutions per minute and the cutting wedge wear of 0.22 mm, the cutting system is stable. The phase

trajectories, being rearranged at each period, are pulled together to some established periodic process, outwardly resembling an invariant torus.

The Mikhailov vector hodograph, for the case of modeling a cutting system with a processing speed of 800 revolutions per minute and a wear value of 0.22 mm, is shown in Figure 6. Here it should be noted that as a result of the hodograph dependence on the frequency, which varies in a wide range from 0 to 4000 Hz, it is impossible to consider the hodograph in one figure, as the events occurring at low frequencies will be invisible due to the scale of events at high frequencies. Based on this, the Mikhailov vector hodograph will be represented by two figures, the first figure reflects events at frequencies up to 1400 Hz, the second- at frequencies above this frequency.

As can be seen from Figure 6, the hodograph of the Mikhailov vector, for the case of a stable cutting system, begins with the positive part of the real axis, rotating around the origin in the direction opposite to the clockwise movement, never turning to zero, sequentially passes  $n$  quadrants, where  $n$  is the order of the differential equation or the order of characteristic polynomial of the system. Thus, the analysis of Figure 6 shows that to analyze the stability of the cutting system, it is sufficient to use the Mikhailov criterion, while relying on the determinant of the linearized system given by the expression (14).

The stability limit of the cutting control system, for the case of processing at a speed of 820 revolutions per minute, is achieved with a wear value along the back face of 0.335 mm, the results of modeling the Mikhailov hodograph for this case are shown in Figure 7.

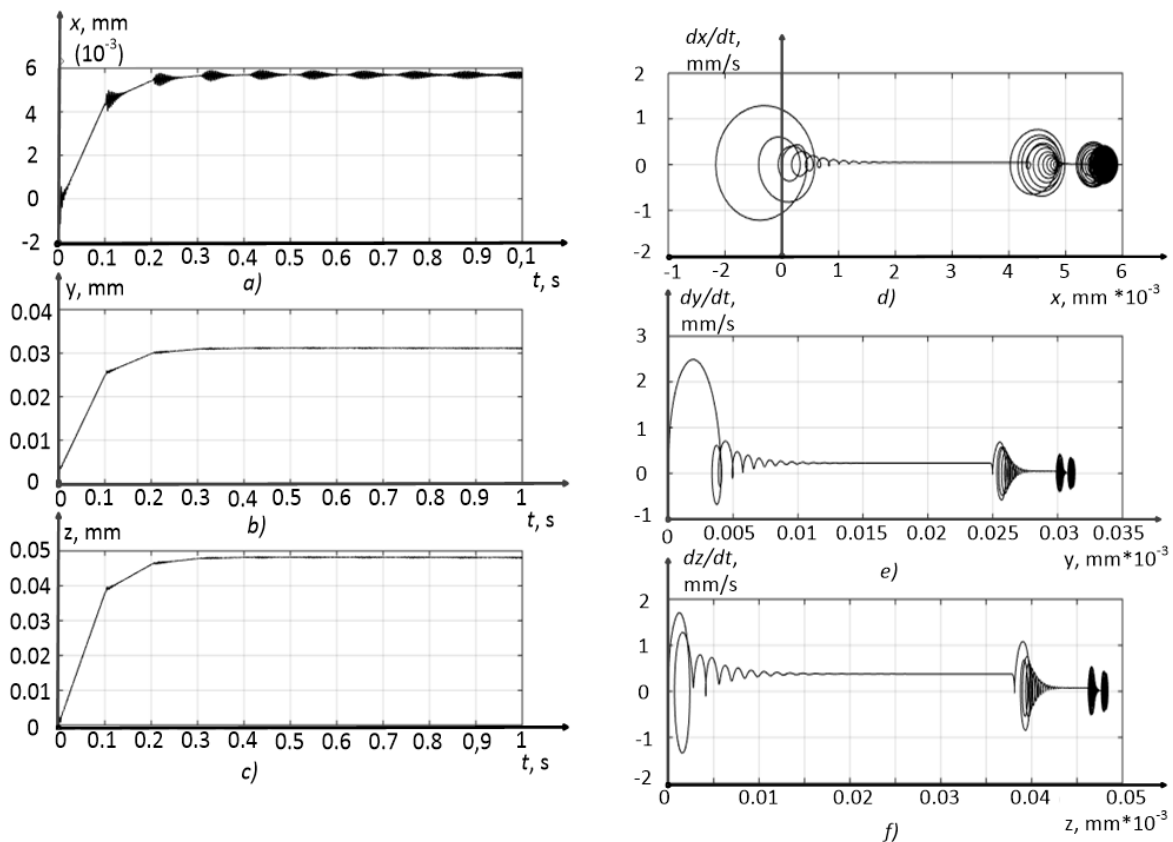


**Figure 5.** For the case of wear  $h=0.22$ : a) x-coordinate deformations, b) y-coordinate deformations, c) z-coordinate deformations, d) x-coordinate phase trajectory, e) y-coordinate phase trajectory, f) phase trajectory, along the z-coordinate

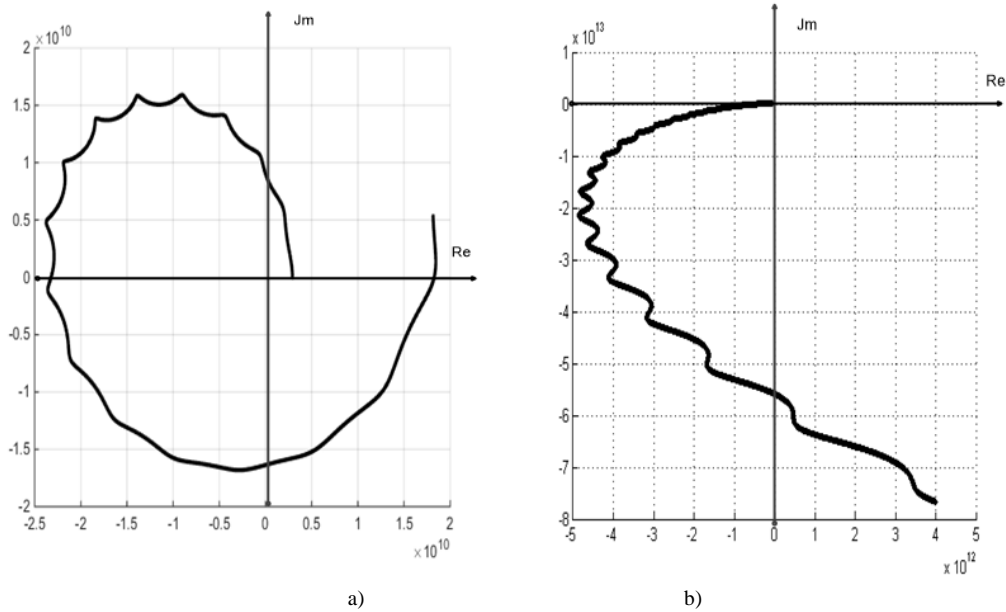


**Figure 6.** The Mikhailov vector hodograph, stable system: a) The beginning of the Mikhailov vector, b) The end of the Mikhailov vector

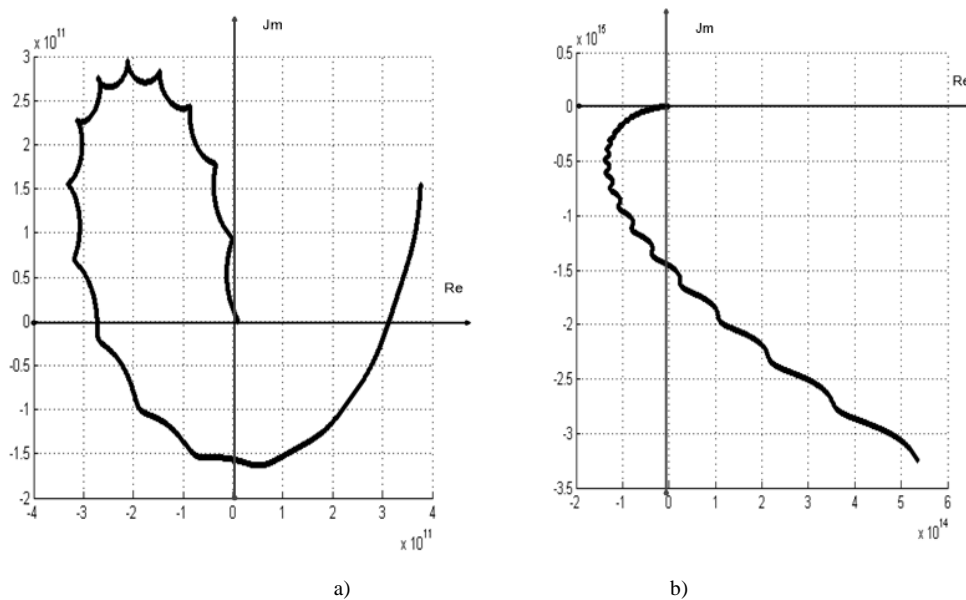


**Figure 7.** The hodograph of the Mikhailov vector, the boundary of the stability of the system: a) The beginning of the Mikhailov vector, b) The end of the Mikhailov vector

As can be seen from Figure 7, the mechanism for displaying the loss of stability by the cutting system, for the case of processing at a speed of 820 revolutions per minute and a wear value of 0.335 mm, consists in the fact that the beginning of the Mikhailov vector shifts to the origin, in addition there is another touch point of the imaginary axis hodograph. This touch point shows the possibility of returning the characteristic from the second quadrant to the first, which would be a violation of the Mikhailov criterion.

An example of an unstable version of the cutting control system, for the case of processing at a speed of 820 revolutions per minute and a wear value of 0.5 mm, is shown in Figure 8.

The maximum stability of the cutting control system according to the criterion of wear of the cutting wedge is observed at a processing speed of 1620 revolutions per minute, it should be noted that this value is close to the calculated value

of the processing speed obtained by analyzing the regeneration of vibrations in this system [Link from metal processing]. However, despite the fact that the maximum value is close to the optimal value determined by the regeneration of vibrations, it is still lower, moreover, there are no subsequent significant spikes in the stability region characteristic of the regeneration of vibrations in the cutting system. It means that changes in the model of the cutting system, the introduction of an additional thermodynamic equation into it and the formation through this equation of a positive feedback on the value of the pushing force distorts the regenerative nature of self-excitation of the cutting tool vibrations.

For further analysis of the cutting control system, we will form into one table all the data obtained in experiments on the upper limit of the stability of the cutting control system according to the Mikhailov criterion (see Table 2).



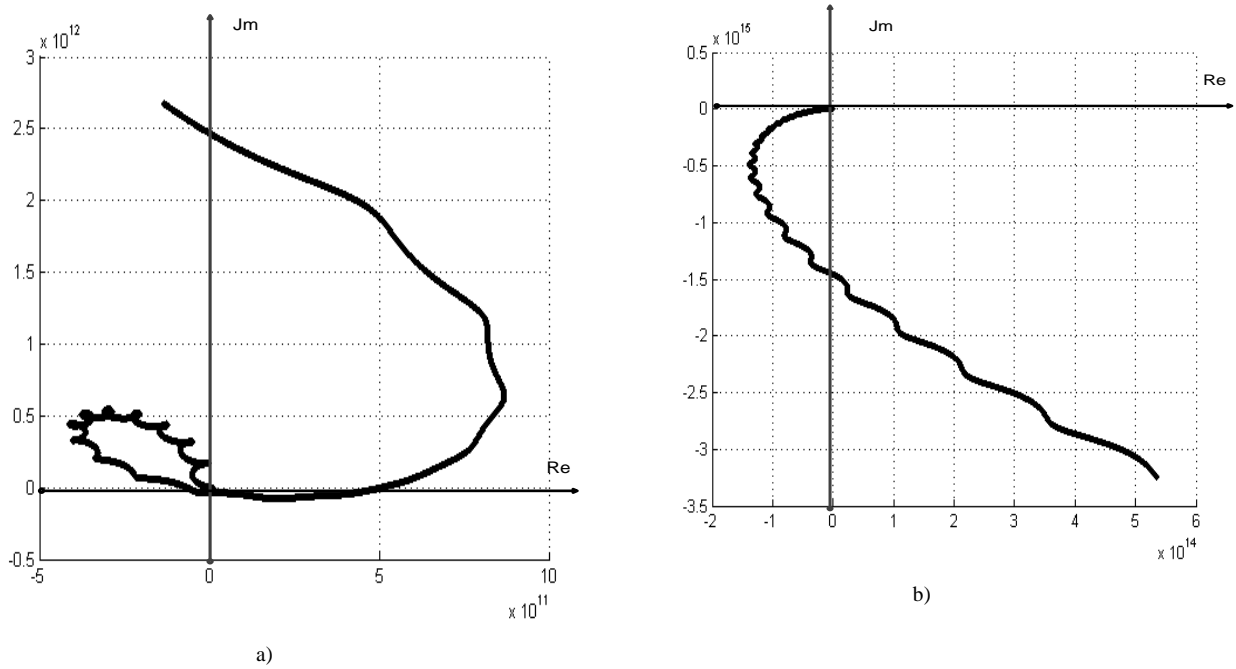


**Figure 8.** The Mikhailov vector hodograph, unstable system: a) The beginning of the Mikhailov vector, b) The end of the Mikhailov vector

**Table 2.** Stability limit of the cutting system

$h_3$ (mm)	0.3	0.31	0.32	0.33	0.335	0.342	0.351	0.36	0.375	0.386
n(rev/min)	360	460	660	760	820	900	1000	1100	1200	1300
$h_3$ (mm)	0.397	0.41	0.43	0.46	0.47	0.44	0.43	0.42	0.418	0.41
n(rev/min)	1400	1500	1560	1600	1620	1680	1700	1750	1800	1900

It can be seen from Table 2 that the maximum of the stability of the cutting control system, in the space of the parameters of the processing speed and the amount of wear of the cutting wedge, is observed at a processing speed of 1620 revolutions per minute. At this point, the amount of wear allowed from the point of view of ensuring the stability of the cutting process was 0.47 mm, which is significantly higher than the average value for the sample, which was  $h \approx 0.39$  mm.

Graphically, the interpretation of the data given in Table 1 is shown in Figure 9.

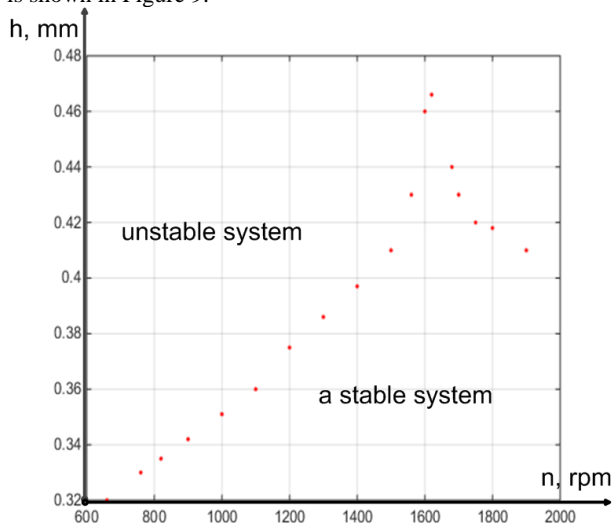


**Figure 9.** Areas of stable and unstable dynamics of the cutting control system

As can be seen from Figure 9, in the area of the studied parameters of the cutting control system, it really has a

pronounced local maximum at a processing speed of 1620 revolutions per minute. Subsequently, there is a decrease in the boundary of the stability area, all this correlates well with the position put forward by A.D. Makarov [22]. At the same time, the increase in the stability limit of the cutting control system is explained by the influence of the temperature-speed factor [23], which is represented in the mathematical model by the expression (1). As can be seen from this expression, the coefficient (the coefficient characterizing the chip pressure on the front face of the cutting wedge) tends to stabilize the drop, and at cutting speeds above 1600 rpm, it does not decrease significantly. The value of the pushing force described by expression (4) continues to grow, with the increasing processing speed, the power of irreversible transformations increases, converted into contact temperature through the equation (10). In other words, there will be a restructuring of the cutting system, in which the cutting force will change slightly, and the pushing force will increase significantly. Such a restructuring leads to the loss of stability of the cutting control system, which is confirmed by a series of field experiments, the results of which are given in [9].

To verify the proposed assumption about the significant effect of the adjustment of the force reaction from the cutting process on the stability of the shaping movements of the tool, let us consider the force reaction at a processing speed higher than the optimal value identified in Figure 9. The results of modeling the forces decomposed along the axes of deformation for the case of processing at the speed of 1700 revolutions per minute and wear values of 0.22 mm and 0.43 mm (the boundary of the stability of the cutting system) are shown in Figure 10.

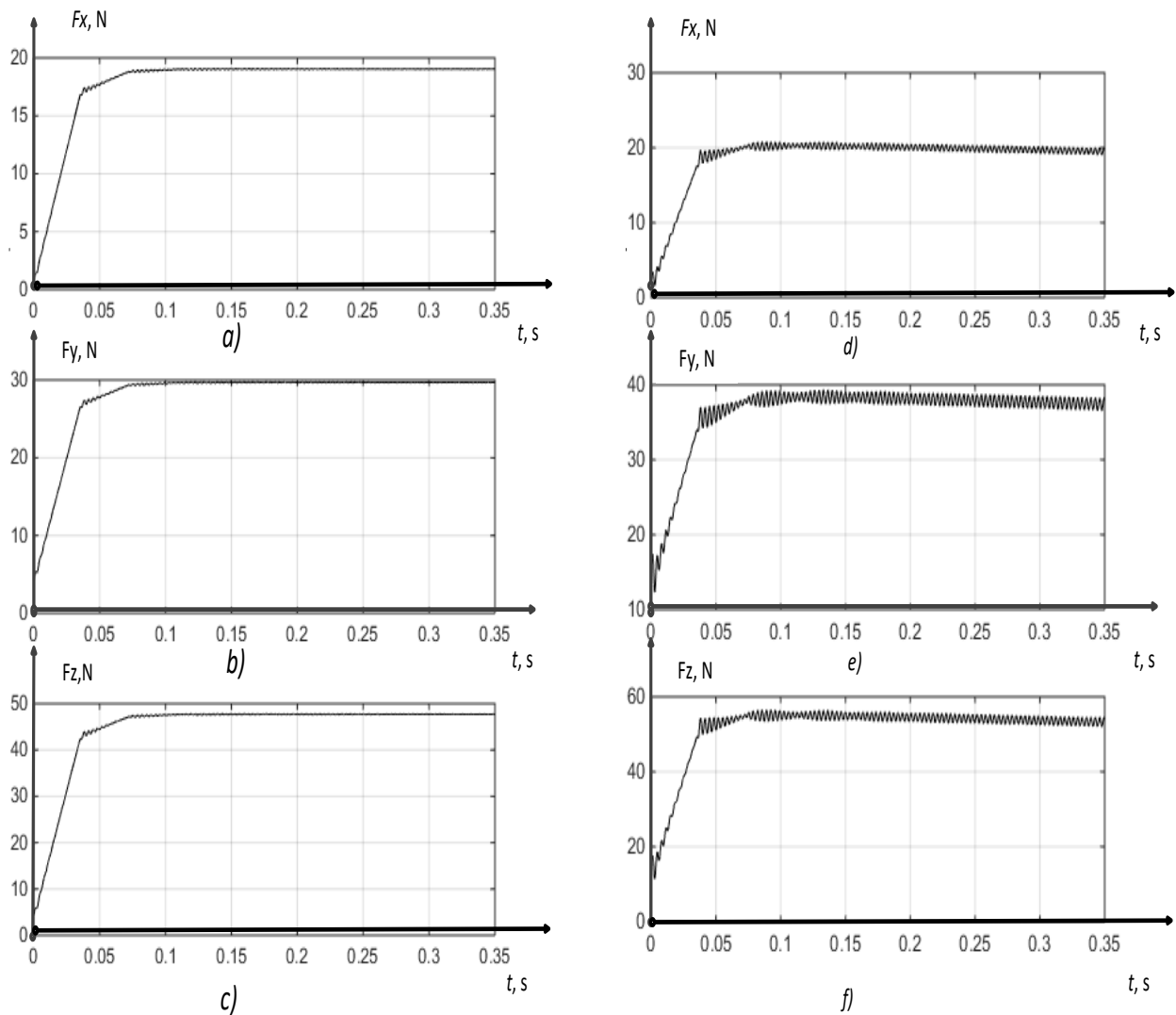


**Figure 10.** Forces for a variant with a processing speed of 1700 rpm : a)  $F_f$  for  $h=0.22$ , b)  $F_p$  for  $h=0.22$ , c)  $F_c$  for  $h=0.22$ , d)  $F_f$  for  $h=0.43$ , e)  $F_p$  for  $h=0.43$ , f)  $F_c$  for  $h=0.43$

As can be seen from Figure 10, with the increase in the amount of wear of the cutting wedge, there is a significant restructuring of the force reaction of the cutting system, the  $F_r$  component increases by 5%, the  $F_p$  component increases by 32%, and  $F_c$  -by 14%. For the case of processing at the speed of 1900 revolutions per minute, the average component of  $F_p$ , with a wear value of 0.41 mm, increases by 38%, which exceeds the average value of  $F_p$  calculated for the results of the experiment shown in Figure 10.

Thus, the restructuring of the reaction forces due to the increase in the pushing force stops the growth of the upper boundary of the stability area of the cutting control system with the further increase in the processing speed after the maximum of the stability area.

Many works have been devoted to the study of the stability of the cutting process, but nowhere before has the influence of the ejecting composing reaction forces been taken into account. It is taking into account this component of the reaction force that allows us to talk about the scientific novelty of the study, its main difference from all previous works.

#### 4. Conclusion

The optimal value of the cutting speed (cutting temperature), when modeling dynamics of processing processes is determined by a combination of the following factors: the incident characteristic of the cutting force, the minimum coefficient of friction due to the transition of friction from adhesive to diffusion nature and the dependence of the force pushing the tool from the preheating of the processing zone, which is due to thermodynamic feedback. However, it should be added here that another important factor determining the optimality of the cutting process is the regenerative effect inherent in the model of the cutting control system, which also has a significant impact on the stability of the dynamics of the cutting system.

All this taken together allows us to formulate the following scientific position: the most optimal mode, in terms of processing speed (cutting temperature), will be a mode with a cutting force close to the minimum, the coefficient of friction will be in some proximity to its local minimum, and the force pushing the tool will not exceed a certain set value, while the speed of cutting will fall into one of the petals of the regenerative effect stability.

## References

- [1] G. Stépán, "Modelling nonlinear regenerative effects in metal cutting". Philosophical Transactions of the Royal Society of London. Series A: Mathematical, Physical and Engineering Sciences, Vol. 359, No. 1781, 2001, 739-757.
- [2] G. Litak, "Chaotic vibrations in a regenerative cutting process". Chaos, Solitons & Fractals, Vol. 13, No. 7, 2002, 1531-1535.
- [3] G. Bolar, "3D Finite Element Method Simulations on the Influence of Tool Helix Angle in Thin-Wall Milling Process". Jordan Journal of Mechanical & Industrial Engineering, Vol. 16, No. 2, 2022, 283-289.
- [4] P. Wahi, A. Chatterjee, "Regenerative tool chatter near a codimension 2 Hopf point using multiple scales". Nonlinear Dynamics, Vol. 40, No. 4, 2005, 323-338.
- [5] S. K. Tiwari, R. K. Singh, B. Kumar, "Optimizing PM Intervals for Manufacturing Industries Using Delay-time Analysis and MOGA". Jordan Journal of Mechanical and Industrial Engineering, Vol. 16, No. 3, 2022, 227-332.
- [6] M. Tomov, B. Prangoski, P. Karolczak, "Mathematical Modelling and Correlation Between the Primary Waviness and Roughness Profiles During Hard Turning". Jordan Journal of Mechanical and Industrial Engineering, Vol. 15, No. 3, 2021, 243-249.
- [7] A. M. Gousskov et al. Nonlinear dynamics of a machining system with two interdependent delays // Communications in Nonlinear Science and Numerical Simulation, Vol. 7, No. 4, 2002, 207-221.
- [8] V. P. Lapshin, "Turning tool wear estimation based on the calculated parameter values of the thermodynamic subsystem of the cutting system". Materials, Vol. 14, No. 21, 2021, 6492.
- [9] V. P. Lapshin, V. V. Khristoforova, S. V. Nosachev, "Relationship of temperature and cutting force with tool wear and vibrations in metal turning" Metal. Work. Mater. Sci., Vol. 22, No. 3, 2022, 44-58.
- [10] V. L. Zakovorotny, V. E. Gvindjiliya, "Evolution of the dynamic cutting system with irreversible energy transformation in the machining zone". Russian Engineering Research, Vol. 39, No. 5, 2019, 423-430.
- [11] V. L. Zakovorotny, V. E. Gvindjiliya, "Correlation of attracting sets of tool deformations with spatial orientation of tool elasticity and regeneration of cutting forces in turning". Izvestiya VUZ. Applied Nonlinear Dynamics, Vol. 30, No. 1, 2022, 37-56.
- [12] Y. Liu, L. He, S. Yuan, "Wear Properties of Aluminum Alloy 211z. 1 Drilling Tool". Jordan Journal of Mechanical and Industrial Engineering, Vol. 15, No. 1, 2021, 59-63.
- [13] V. P. Astakhov, "The assessment of cutting tool wear". Int. J. Mach. Tools Manuf., Vol. 44, No. 6, 2004, 637-647.
- [14] F. Zeqiri, B. Fejzaj, "Experimental Research and Mathematical Modeling of Parameters Affecting Cutting Tool Wear in Turning Process of Inconel 625". JJMIE, Vol. 16, No. 5, 2022, 787-792.
- [15] A. Pereda, L. A. Vielva, A. Vegas, A. Prieto, "Analyzing the stability of the FDTD technique by combining the von Neumann method with the Routh-Hurwitz criterion". IEEE Transactions on Microwave Theory and Techniques, Vol. 49, No. 2, 2001, 377-381.
- [16] L. Kolev, S. Petrakieva, "Interval Raus criterion for stability analysis of linear systems with dependent coefficients in the characteristic polynomial". IEEE, Vol. 1, 2004, 130-135.
- [17] V. L. Zakovorotny, V. E. Gvindjiliya, "Correlation of attracting sets of tool deformations with spatial orientation of tool elasticity and regeneration of cutting forces in turning". Izvestiya VUZ. Applied Nonlinear Dynamics. Vol. 30, No. 1, 2022, 37-56.
- [18] T. R. Velieva, D. S. Kulyabov, A. V. Korolkova, I. S. Zaryadov, "The approach to investigation of the the regions of self-oscillations". VI International Conference Problems of Mathematical Physics and Mathematical Modelling, Moscow, Russian Federation, 2017.
- [19] P. Sourdille, A. O'Dwyer, E. Coyle, "Smith predictor structure stability analysis using Mikhailov stability criterion". Proceedings of the 4th Wismarer Automatisierungs Symposium, Wismar, Germany, 2005
- [20] A. I. Saleh, M. M. M. Hasan, N. M. M. Darwish, "The Mikhailov stability criterion revisited". JES. Journal of Engineering Sciences, Vol. 38, No. 1, 2010, 195-207.
- [21] L. K. Barker, "Mikhailov stability criterion for time-delayed systems". №. NASA-TM-78803, 1979, 1-17.
- [22] A. D. Makarov. Optimizaciya processov rezaniya [Optimization of cutting processes]. Moscow: Engineering; 1976.
- [23] M. Soori, M. Asmael, "A review of the recent development in machining parameter optimization". Jordan Journal of Mechanical and Industrial Engineering, Vol. 16, No. 2, 2022, 205-223.